Egyptian Journal of Radiology and Nuclear Medicine

RESEARCH

Open Access

Validity of dynamic contrast-enhanced magnetic resonance imaging of the breast versus diffusion-weighted imaging and magnetic resonance spectroscopy in predicting the malignant nature of non-mass enhancement lesions

Dalia Bayoumi[1], Farah Ahmed Shokeir[1], Rasha Karam[1] and Aya Elboghdady[1*]

Abstract

Background Breast cancer is the commonest cancer affecting women worldwide. So, it is important to accurately detect and classify different breast lesions. Noninvasive methods for tissue characterization have increased interest, particularly for early diagnosis. Non-mass enhancement (NME) breast lesions are described in magnetic resonance imaging (MRI) as the presence of enhancement without space-occupying lesions. Several studies have described that certain characteristics can be used as new indicators of malignancy in breast NME lesions. We aimed to study the role of multiparametric-MRI (Mp-MRI) as diffusion-weighted imaging (DWI) and magnetic resonance spectroscopy (MRS) in assessment of NME lesions and to suggest which one offers the greatest diagnostic accuracy.

Methods This retrospective study was conducted from March 2017 to December 2023 on 220 NME breast lesions. All lesions were analyzed to study the features of benign and malignant NME lesions using different MRI techniques including dynamic contrast-enhanced MRI (DCE-MRI), DWI, and MRS. Breast MRI was performed at 1.5 Tesla, findings were correlated with histopathological results of all cases.

Results Patients' mean age was 46.56 years with 220 NME breast lesions (54 were benign and 166 were malignant). Invasive ductal carcinoma with ductal carcinoma in situ was the most malignant type representing 93 cases. We found that segmental distribution, heterogeneous enhancement, type III curve, restricted diffusion, lower apparent diffusion coefficient, and positive choline peak were more with malignancy ($P = 0.008$, 0.02, 0.004, 0.001, and < 0.001). We detected that Mp-MRI has higher diagnostic accuracy than DCE-MRI and combined other functional sequences (DWI, MRS), it was 91.2% with sensitivity 89.9%, specificity 87.8%, positive predictive value 89.2%, and negative predictive value 82.2%.

Conclusions Functional MRI techniques, such as DWI and MRS, can provide helpful information in assessment of NME lesions. They have high diagnostic accuracy, sensitivity, and specificity in characterizing NME breast lesions as benign or malignant. However, DCE-MRI is mandatory for lesion characterization and delineation of its nature

*Correspondence:
Aya Elboghdady
ayabogdady@mans.edu.eg
Full list of author information is available at the end of the article

and cannot be replaced by them alone in cases of lesion visualization. So, multiparametric-MRI can improve the diagnostic accuracy of NME breast lesions when combined with dynamic contrast-enhanced MRI and can help in reducing negative biopsy rates.

Keywords Breast cancer, MRI breast, Time–intensity curve, Non-mass enhancement lesions, DWI, MRS, Multiparametric-MRI

Background

Breast cancer is the most widespread cancer affecting women worldwide. Every year, around 1.5 million women are diagnosed with breast cancer. Therefore, it is important to accurately detect and classify different breast lesions to determine the most effective treatment plan and prognosis. Noninvasive methods for tissue characterization have gained clinical interest, particularly in the early stages of diagnosis [1].

A non-mass-enhancing lesion on breast ultrasound (US) is a lesion that takes up space in two different sonographic planes but cannot be identified as a mass due to the lack of a clear margin or shape [2].

The incidence of non-mass lesions detected during breast ultrasound screening was 1.0%, with a likelihood of malignancy above 2%. These lesions can be classified as BI-RADS category 4a, and tissue diagnosis is necessary [3].

Non-mass enhancement lesions are typically observed in mammography as either focal asymmetry or calcification which makes it challenging to diagnose them using dynamic and shape characteristics alone [4].

MRI is highly sensitive in identifying breast malignancies. Non-mass enhancement (NME) breast lesions are described in magnetic resonance imaging (MRI) as the presence of enhancement without space-occupying lesions. Previously, radiologists assumed that non-enhancing breast lesions were not malignant due to the principle of tumor angiogenesis [5].

Dynamic contrast-enhanced magnetic resonance imaging (DCE-MRI) is now considered as a very accurate method in detecting breast cancer. It outperforms mammography and ultrasound in women at any risk of breast cancer, with a pooled sensitivity of 93% [6, 7].

Several studies have shown that certain descriptor features, such as segmental distribution pattern, clustered ring pattern of enhancement, and short time to reach the peak level of enhancement, can be used as new indicators of malignancy in breast non-mass enhancement lesions [8].

In order to enhance the accuracy of diagnosis, various additional MRI techniques have been investigated, including proton MR, phosphorus spectroscopy, sodium imaging, and diffusion-weighted imaging (DWI). Among these techniques, DWI has proven to be reliable and beneficial for differentiating benign from malignant breast lesions [9–11].

The diagnostic ability of magnetic resonance spectroscopy (MRS) is essentially based on detecting increased levels of choline-containing compounds (tCho) in malignant breast lesions. This has been shown to differentiate them from benign lesions and enhance the specificity of MRI [12].

Aim of work

To study the role of multiparametric-MRI (Mp-MRI) with diffusion-weighted imaging (DWI) and magnetic resonance spectroscopy in assessment of breast non-mass enhancement lesions & their different types and to suggest which one offers the greatest diagnostic accuracy.

Methods

This is a retrospective study that was approved by the institutional Research Board.

Study population

Between March 2017 and December 2023, all breast lesions were retrospectively analyzed. The inclusion criteria were: (1) the presence of non-mass enhancing lesions (BI-RADS 3–5) on MRI; (2) non-mass enhancing breast lesions with revised histopathological reports, and (3) the presence of accurate clinical details of each case. The exclusion criteria were: (1) any breast lesions delineated as patchy foci (too small < 5 mm) or mass, which is a lesion that occupy a space ≥ 10 mm; (2) breast lesions that underwent any form of treatment before performing MRI scan; and (3) distorted images that we could not assess accurately. At the end, 220 patients having 220 lesions were included in our study and the NME lesions were accurately pathologically diagnosed either by excisional biopsy or ultrasound-guided core needle biopsy (US-CNB). The patients' ages ranged from 30 to 70 years, with a mean age of 50.7 years.

MRI procedure

- All breast MRI scans were conducted on a 1.5 Tesla machine with a dedicated breast coil, with patients in a prone position. The imaging protocol involved a conventional MR study, which included axial T1- and

T2-weighted imaging, with suppression of the signal from adipose tissue by STIR. Additionally, DWI was acquired pre-contrast administration using a multi-section single-shot SE EPI sequence with b values of 0, 500, and 1000 mm^2/sec, including the calculation of the ADC map. Furthermore, dynamic post-contrast imaging was performed using axial GRE-T1-weighted images with the FAT-SAT technique after administration of a contrast agent. A bolus of gadopentetate dimeglumine in a dose of 0.1–0.2 mmol/kg was injected using an automated injector with a rate of 3–5 ml/sec through an 18–20 gauge intravenous cannula inserted in the antecubital vein, followed by a bolus injection of saline (total of 20 ml at 3–5 ml/s). The dynamic study consisted of one pre-contrast and five post-contrast series, each of which took about 1.15 min. After all MRI sequences had been performed, multi-voxel ^{1}H MRS was performed. Proton MRS images were done on a single 10 mm thickness sagittal section using a Point Resolved Spectroscopy Sequence (PRESS) with water & lipid suppression. MRS parameters were TR/TE 2000 m s/272 m s; matrix size 18 X 18; FOV = 18 cm; and total data acquisition time was approximately 12 min.

- Post-processing of images includes creating time-to-signal intensity curves to enhanced lesions and subtracting images in-line using the MIP algorithm in axial, coronal, and sagittal projections. Post-processing of the spectroscopic data was performed by using the manufacturer software to detect choline-containing compounds (Cho) peak. Placement of the MRS Voxel was usually determined by reviewing lesion's morphology and contrast uptake kinetics while the patient is still in the magnet. The position and size of the region of interest (ROI) was chosen to encompass each enhancing lesion limiting as much as possible the inclusion of non-enhancing parenchyma and surrounding fat.

Imaging analysis

The analysis of breast images was carried out by a minimum of two experienced radiologists. They evaluated imaging characteristics of non-mass enhancing lesions (there is no space-occupying effect and lesion is not observed on unenhanced sequences) as regards. (I) Enhancement distribution either focal, linear, segmental, regional, multiple regions, or diffuse. And (II) internal enhancement pattern either homogenous, heterogeneous, clumped, or clustered ring. And enhancement dynamics (kinetics). The signal-to-time curve was defined to assess the enhancement dynamics which was described as type 1 (persistent dynamic curve—more than 10% with time), type 2 (plateau dynamic curve—does not alter following initial rise), or type 3 (washout dynamic curve—reduction of more than 10%) [13]. The lesions were also determined on DWI and ADC map by using the conventional MR images as a guide and were described as either hypointense (free diffusion) or hyperintense (restricted diffusion) according to the intensity of the lesion on DWIs (b 1000). The apparent diffusion coefficient (ADC) values were measured by the machine through putting the ROI within the lesions' borders (not less than three ROIs were used, then the mean ADC value for the lesion was calculated), which was then expressed in 10-^{3}mm^2/s. Apparent cystic or necrotic components were excluded by returning back to the original MR images. Analysis of MRS data and spectrum was performed by calculating the Cho peak from water-suppressed spectrum using a narrow frequency range (e.g., 2.92–3.52 ppm), the choline peak was considered as positive if present at 3.23 ppm and negative if absent.

Statistical analysis

The data were tabulated, coded, and then analyzed using the SPSS version 25.0.

Descriptive statistics were calculated in the form of Mean ± Standard deviation (SD) for quantitative data and frequency (number-percent) for qualitative data.

Analytical statistics: The inter-group comparison of categorical data, the significance of difference was tested using one of the following tests: Student's *t* test, Whitney U test, Chi-square test (χ^2 value) or Fisher's exact test, Shapiro–Wilk's test, Spearman's correlation, binary logistic regression (univariate logistic regression), or multivariate logistic regression.

The sensitivity, specificity, positive predictive value, negative predictive value, and accuracy were calculated. ADC was examined at different cutoff points using receiver operating characteristic (ROC) curve analysis to determine the best cutoff point as well as the diagnostic power of each test. The P value ≤ 0.050 was considered statistically significant. The P value < 0.0001 was considered highly significant in all analyses.

MRI findings have been correlated with standard of reference which is the results of the histopathological studies either after open or closed biopsy.

Results

We enrolled 220 patients with 220 non-mass enhancement lesions. Their ages ranged from 32–82 years old showing no difference in the mean age between benign and malignant lesions (46.54 ± 11.68 and 46.85 ± 11.68, respectively) and their mean difference was statistically insignificant (P value 0.959) as well. Regarding the family history of breast cancer, out of the 220 lesions, 172 had a

negative family history and there was a statistically significant difference between benign and malignant lesions (*P* value 0.001). As regards the clinical data of the included cases, the most common symptomatic presentation was palpable breast mass which represents 160 cases out of the 220 cases included in this study and was distributed between 138 malignant cases and 22 benign cases. Please refer to Table 1 for a detailed demographic of the study population. Out of the 220 NME breast lesions, there were 166 NME malignant lesions and 54 benign lesions. Regarding the histopathological type of the included lesions; as regards the malignant lesions, invasive ductal carcinoma (IDC) with ductal carcinoma in situ (DCIS) was the most common malignant type (Fig. 1) representing 93(42.3%) of the studied cases and ductal carcinoma in situ (Figs. 2 and 3) was the second common malignant type representing 39(17.7%) of the studied cases. As regards the benign lesions, inflammatory changes were the most common benign type representing 44(20%) (Fig. 4) while fibrocystic disease represents 10(4.5%) of the studied cases (Fig. 5). Detailed histopathologic categories of the studied non-mass enhancement breast lesions are shown in Table 2.

MRI imaging analysis

MRI descriptive features of the 220 breast lesions are illustrated in Table 3. Regarding the distribution characteristics of the NME breast lesions; regional, segmental, and multi-regions distributions were found to show significant statistical difference between the benign and malignant breast lesions groups ($P=0.008$, $P=0.001$ & $P=0.001$), respectively. The segmental distribution was encountered more in malignant NME lesions (69/166, 41.6%), while in benign breast lesions it represents (9/54, 16.7%). On the other hand (13/54, 24.1%) of the benign NME lesions displayed linear distribution and (9/166, 5.4%) out of the malignant NME lesions displayed linear distribution pattern. As regards the patterns of internal enhancement, the incidence of heterogeneous enhancement was the most common enhancement seen in malignant lesions, with a prevalence of (75/166, 45.2%) and a PPV of 65.4%, and cluster-ring enhancement was (11/166, 6.6%) in malignancy was not found in benign lesions and this was significant statistically ($P=0.001$). Regarding benign NME lesions, homogenous enhancement was the most common enhancement pattern, which was observed in (35/54, 65.3%) of the benign cases. Of the dynamic curves, the washout type curve (type III) showed statistical significance between benign and malignant non-mass enhancing lesions ($P=0.02$). The washout type curve (type III) was detected more in malignant lesions (97/166, 58.4%), markedly higher than that in the benign group (4/54, 7.4%). The frequency of type I was detected more in benign NME lesions (36/54, 66.7%) than in malignant lesions (22/166, 13.3%). The sensitivity and specificity of the dynamic contrast-enhanced MRI model in predicting malignant lesions were 86.1% and 96.3%. Concerning DWI, restricted diffusion was more commonly detected in malignant cases; observed in (145/166, 87.3%). The sensitivity and specificity of the diffusion-weighted MRI in predicting malignant lesions were 87.8% and 33.3%. Regarding ADC values, we found that malignant non-mass enhancing lesions mostly displayed low ADC values ($\leq 1.03\times10^{-3}$ mm^2/s) compared to benign NME lesions. We found that the best ADC cutoff value to differentiate between benign and malignant lesions was 1.15×10^{-3} mm^2/s, and their difference was significant statistically (P value $=0.002$) (Fig. 6). The sensitivity and specificity of the ADC value ($\leq 1.03\times10^{-3}$ mm^2/s) for detecting malignant NME lesions were 70.3% and 41.7%. As regards MRS findings; out of 166 malignant NME lesions 142(85.5%) showed positive choline peak, and this was statistically significant compared to the benign NME lesions ($P<0.001$). The sensitivity and specificity of the positive choline peak for detecting malignancy were 85.5% and 72.2%. We studied

Table 1 Baseline demographics

Parameter	Total cases N = 220 Frequency (%)	Benign N = 54, 24.5%	Malignant N = 166, 75.5%	Test of significance
Average patient age	46.56 ± 10.87	46.54 ± 11.68	46.85 ± 11.68	t = 0.051, P = 0.959
Family history: Negative	172(78.2%)	54(100%)	118(71.1%)	$\chi^2 = 19.97$, $P = 0.001$*
Positive	48(21.8%)	0	48(28.9%)	
Presentation type:				
Screening	8(3.6%)	6(11.2%)	2(1.2%)	$\chi^2 = 8.86$, P = 0.009*
Symptomatic: Palpable lesion	160(72.7%)	22(40.7%)	138(83.1%)	$\chi^2 = 86.49$, P < 0.001*
Bloody nipple discharge	22(10%)	0	22(13.2%)	$\chi^2 = 10.86$, P = 0.001*
Mastalgia	30(13.7%)	26(48.1%)	4(2.5%)	$\chi^2 = 73.4$, P < 0.001*

t Student's t test, χ^2 Chi-Square test, *P* Probability, *Statistically significant

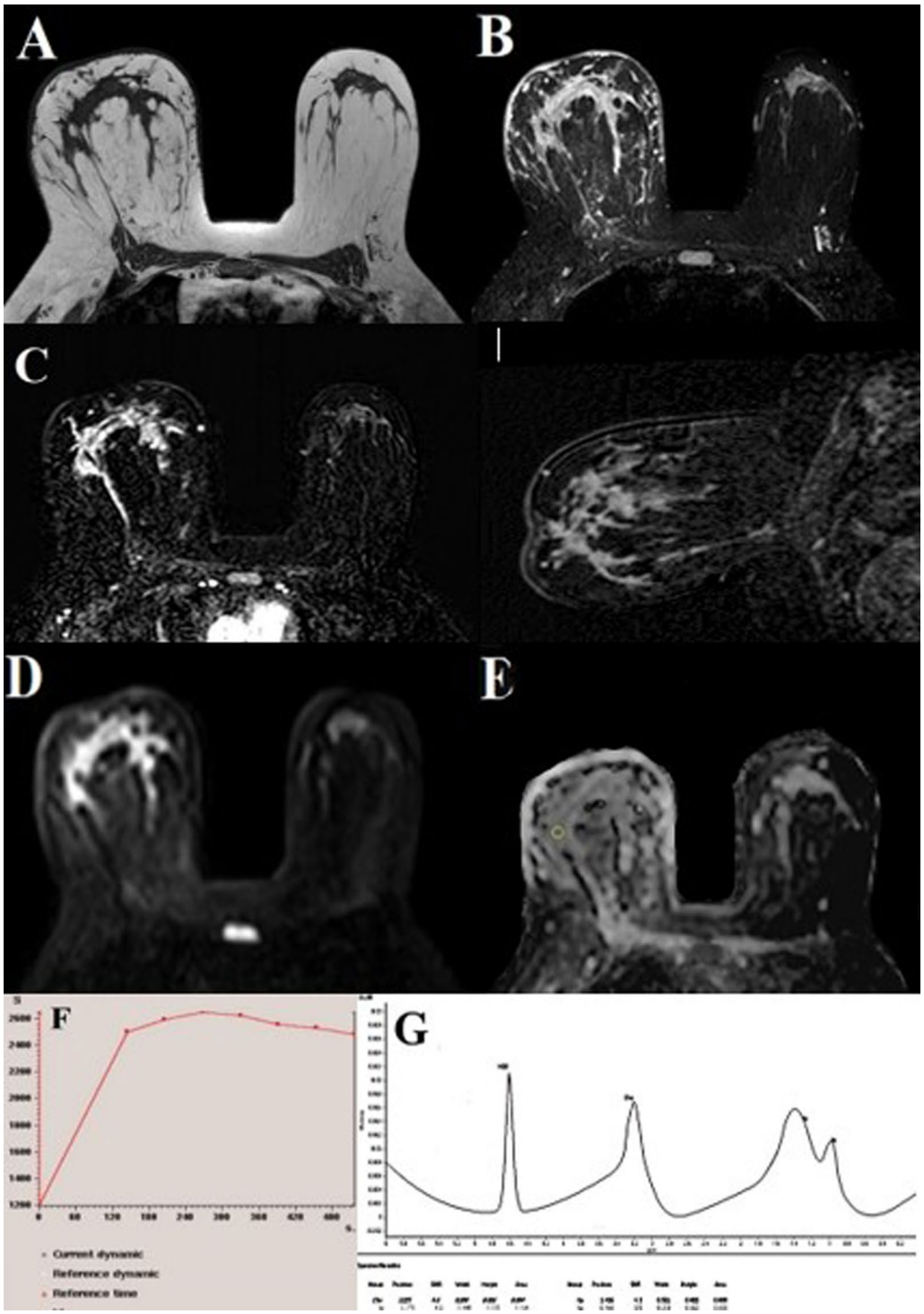

Fig. 1 Female patient aged 42 years old complaining from right palpable lump. MRI revealed: **A** Pre-contrast T1-weighted axial image: showing an ill-defined area of tissue distortion displaying low signal intensity involving mainly the central area of the right breast. **B** STIR axial image: showing large area of central tissue distortion extending to right upper outer quadrant displaying high signal intensity. **C** Post-contrast subtraction axial and sagittal images: showing heterogeneous multicentric non-mass enhancement is seen diffusely distributed in right breast parenchyma along with enhanced retro-areolar ducts with thick enhanced overlying skin. **D** and **E** DWI shows high signal and low signal in ADC map, with mean ADC value = 0.9 $\times 10^{-3}$ mm/s. **F** The enhancement kinetic curve of the lesion shows type III washout curve. **G** MRS revealed positive choline peak. Pathology proved to be Grade III invasive ductal carcinoma with low-grade ductal carcinoma in situ (DCIS)

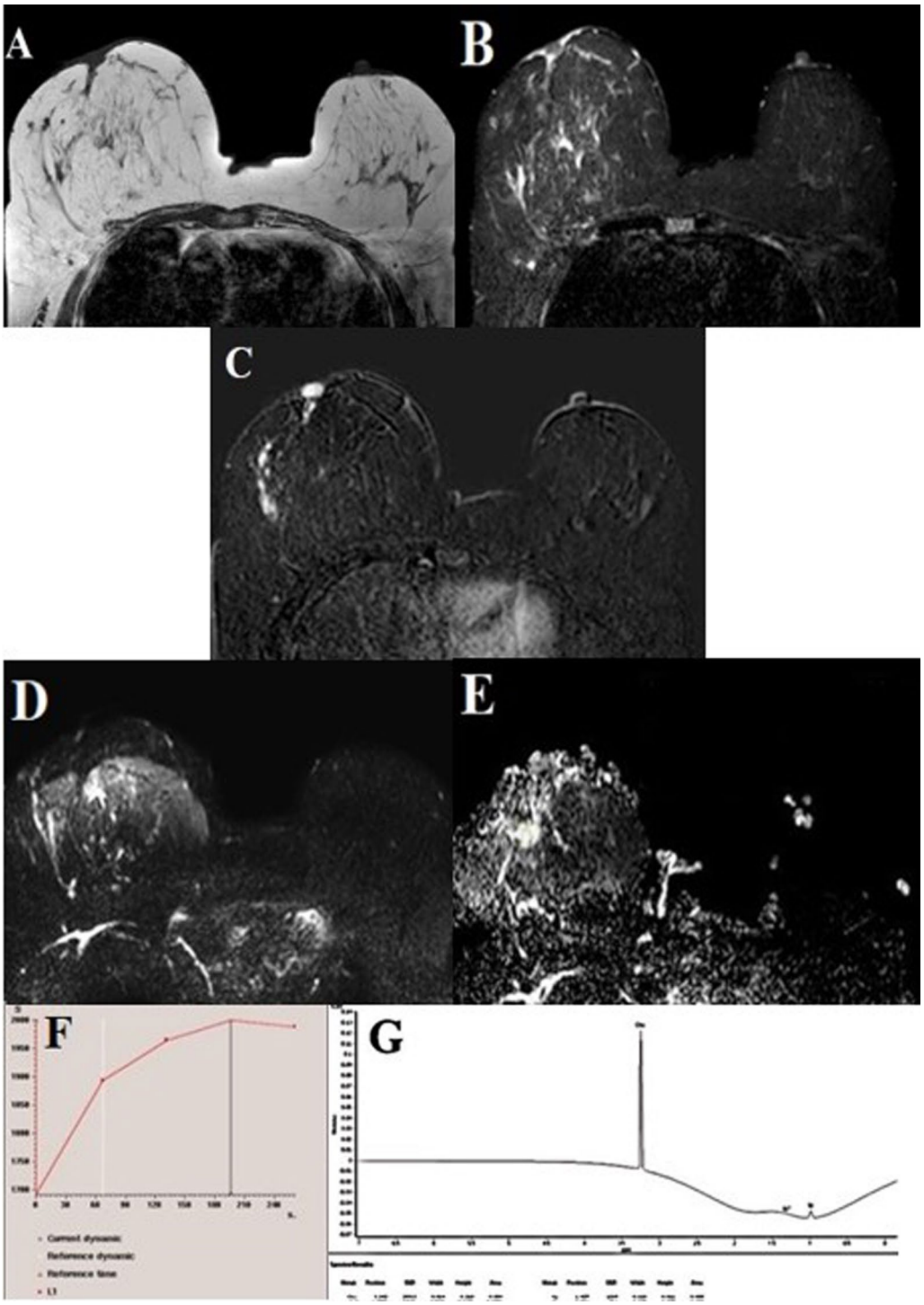

Fig. 2 Female patient aged 45 years old complaining from nipple discharge and skin changes. MRI revealed: **A** Pre-contrast T1-weighted axial image showing: Retracted nipple. **B** STIR axial image showing: an area of tissue distortion displaying intermediate signal intensity is seen at the upper outer quadrant of the right breast and extending to nipple areolar complex. **C** Post-contrast subtraction axial images showing: linear clumped non-mass enhancement involving nipple areolar complex with subsequent nipple inversion and abnormal nipple enhancement. **D** and **E** DWI of the lesion showing: high signal intensity with low signal in ADC map with mean ADC value measured at nipple areolar complex = 0.6×10^{-3} mm/s. **F** The enhancement kinetic curve of the lesion is type III washout curve. **G** MRS revealed: positive choline peak. Pathology proved to be high-grade ductal carcinoma in situ (Paget's disease of the nipple)

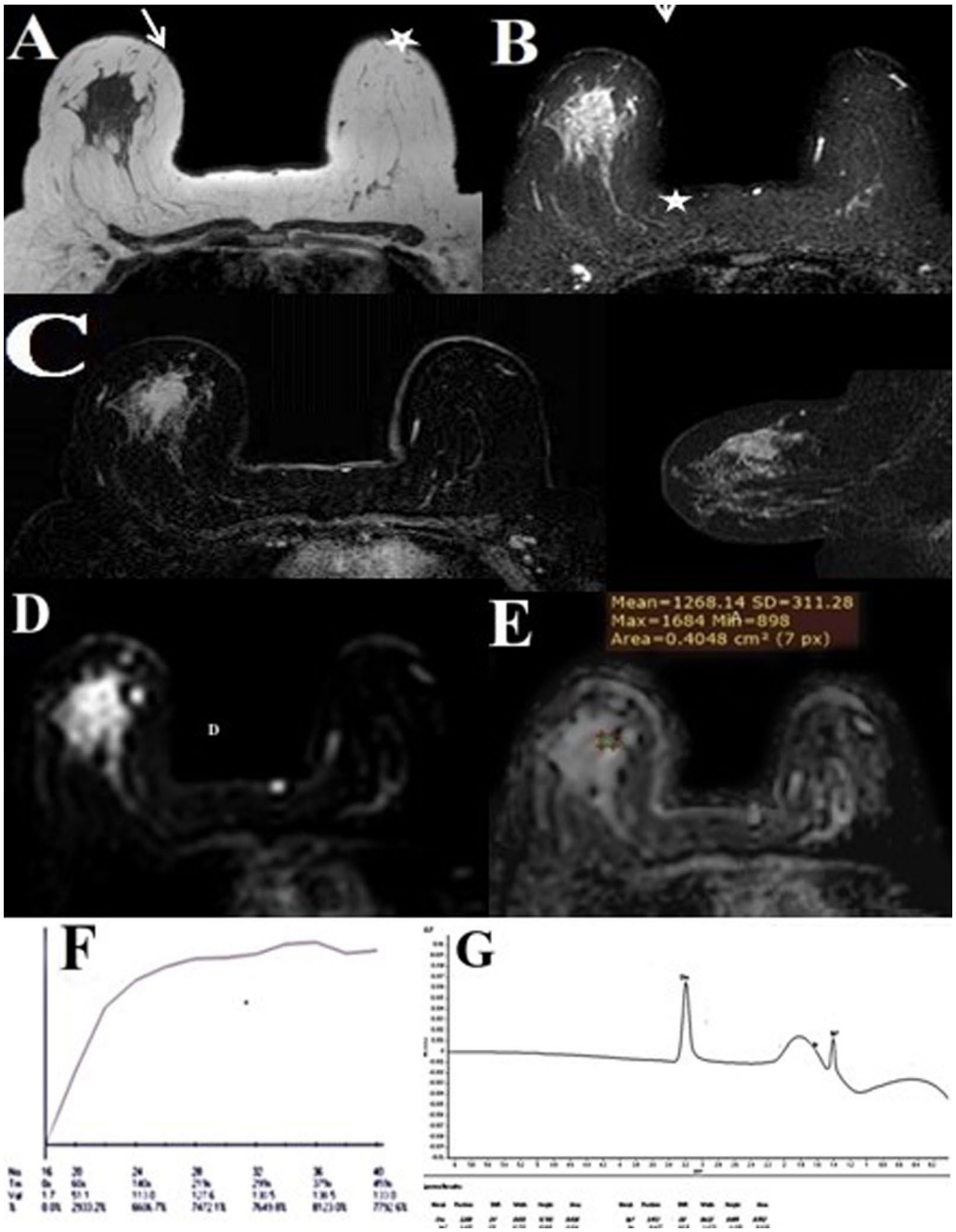

Fig. 3 Female patient aged 53 years old complaining from right mastalgia. MRI showed: **A** Pre-contrast T1-weighted axial image showing: multiple non-circumscribed areas of tissue distortion displaying low signal intensity at the upper half of the right breast. **B** STIR axial image showing: scattered areas of high signal intensity. The largest area is still observed in the upper half of the right breast. **C** Post-contrast subtraction axial and sagittal images: showing regional heterogeneous non-mass enhancement in the upper half of the right breast. **D** and **E** DWI showing: high signal intensity with low signal in ADC map with mean ADC value = 1.26×10^{-3} mm/s. **F** The enhancement kinetic curve: type II plateau curve. **G** MRS: revealed positive choline peak. Pathology revealed: multi-centric high-grade ductal carcinoma in situ (DCIS) with foci of microscopic invasion

the diagnostic accuracy of combined functional MRI techniques (DWI, ADC, and MRS) without DCE-MRI, it was 85% with a sensitivity of 85.5%, specificity of 83.3%, PPV of 94%, and NPV of 65.2%. And it also assessed the diagnostic accuracy of multiparametric-MRI including (DCE-MRI, DWI, ADC, and MRS) which was 91.2% with a sensitivity of 89.9%, specificity of 87.8%, PPV of 89.2%, and NPV of 82.2% demonstrating significant

improvement. Table 4 summarizes the diagnostic accuracy of various MRI techniques in predicting malignant non-mass enhancement lesions.

Discussion

Breast cancer is a major cause of illness and death among women around the world. Detecting and treating all types of cancer early is important for a better chance of recovery. Women who are diagnosed with small tumors' size have a much higher chance of surviving the disease [14].

Imaging is essential for breast cancer screening, diagnosis, preoperative/treatment assessment, and follow-up [15].

Multiparametric-MRI (Mp-MRI) is an innovative approach that enhances the specificity of DCE-MRI. It involves combining established functional parameters such as diffusion-weighted imaging (DWI) and MR spectroscopy (MRS). This combination of parameters provides a better understanding of breast cancer development and disease progression. Additionally, it enables a more accurate assessment of treatment response by quantifying physiological and pathological processes at the cellular level. This technique has the potential to be groundbreaking in the field of breast cancer diagnosis and treatment [16].

Our study included 220 female patients with non-mass enhancement lesions, their mean age (46.56 ± 10.87) with a range from 30 to 82 years. Regarding the clinical data of the studied cases, the most common warning sign was palpable mass specifically in malignant cases more than benign cases 138 out of 166 malignant NME lesions ($P < 0.001$). These findings are consistent with a study conducted by Park and his colleagues who reported that palpability was frequently detected in patients with malignant non-mass enhancing lesions than in those with benign non-mass enhancing lesions ($P = 0.000$) [17].

Family history is one of the most important factors that have a major impact on the risk of having breast cancer. Approximately 15% of breast cancer patients have relatives diagnosed with breast cancer and the risk of disease developing increases by two- to threefold, especially with a history of breast cancer in their first-degree relatives this was reported by a study conducted by Liu and his colleagues**.** In our study, a positive family history of breast cancer in first- and second-degree relatives was detected in 48(28.9%) out of 166 malignant cases [18].

Our study showed that malignant lesions were the predominant pathological finding, with 75.5% (166/220) of the NME lesions detected on DCE-MRI being malignant, while the remaining 24.5% (54/220) were benign. These results are consistent with a study conducted by Marino and his colleagues which found that malignant non-mass enhancing lesions accounted for 59% of cases, while benign lesions accounted for 41% [10].

Our analysis also revealed that invasive ductal carcinoma (IDC) with DCIS component (93 cases) and ductal carcinoma in situ (DCIS) (39 cases) were the most common malignant non-mass pathologies. This finding is in agreement with a study by Huang and his colleagues which reported that the final pathology in malignant non-mass enhancing lesions showed that 58.7% (132/225) of patients had both invasive cancer and DCIS component, 26.7% had invasive cancer only, and 7.6% had DCIS only Additionally, Mori and colleagues reported that non-mass enhancing lesions were the most common manifestation of ductal carcinoma in situ (DCIS) and invasive ductal carcinoma with an extensive intraductal component, although there are multiple benign abnormalities appear as non-mass enhancing lesions. Consequently, non-mass enhancing lesions contribute to false-positive breast MRI findings, often leading to needed biopsy [19, 20].

In terms of the distribution of non-mass enhancing lesions, our study found that the majority of malignant lesions (69/166, 41.6%) had a segmental distribution ($P = 0.001$). On the other hand, linear distribution was commonly found in benign lesions (13/54, 24.1%), which was higher than its frequency in malignant lesions (9/166, 5.4%). These findings are consistent with previous studies by Liu, Asada, Aydin, and their colleagues who also discovered that the segmental pattern of distribution was predominant in malignant non-mass enhancing lesions ($P = 0.001$), while the linear pattern of distribution was more associated with benign NME lesions ($P = 0.002$) and with less association with malignancy and also our results

(See figure on next page.)

Fig. 4 Female patient aged 39 years old complaining from left mastalgia and bloody nipple discharge. MRI revealed: **A** Pre-contrast T1-weighted axial image showing ill-defined area of low signal intensity seen at upper outer quadrant (UOQ) of the left breast reaching the nipple areolar complex. **B** STIR axial image showing ill-defined area of mixed intermediate and high signal intensity seen at UOQ of the left breast reaching the nipple areolar complex. **C** Post-contrast subtraction axial & sagittal images showing heterogeneous non-mass enhancement with segmental distribution seen at UOQ of the left breast reaching the nipple areolar complex with related dilated thick-walled enhancing retro and peri-areolar ducts. **D** and **E** DWI of the lesion showing high signal intensity with mean ADC value = 1.58×10^{-3} mm/s. **F** The enhancement kinetic curve of the lesion is progressive enhancement type I curve. **G** MRS revealed a negative choline peak. Pathology proved to be benign duct ectasia and peri-ductal chronic inflammation

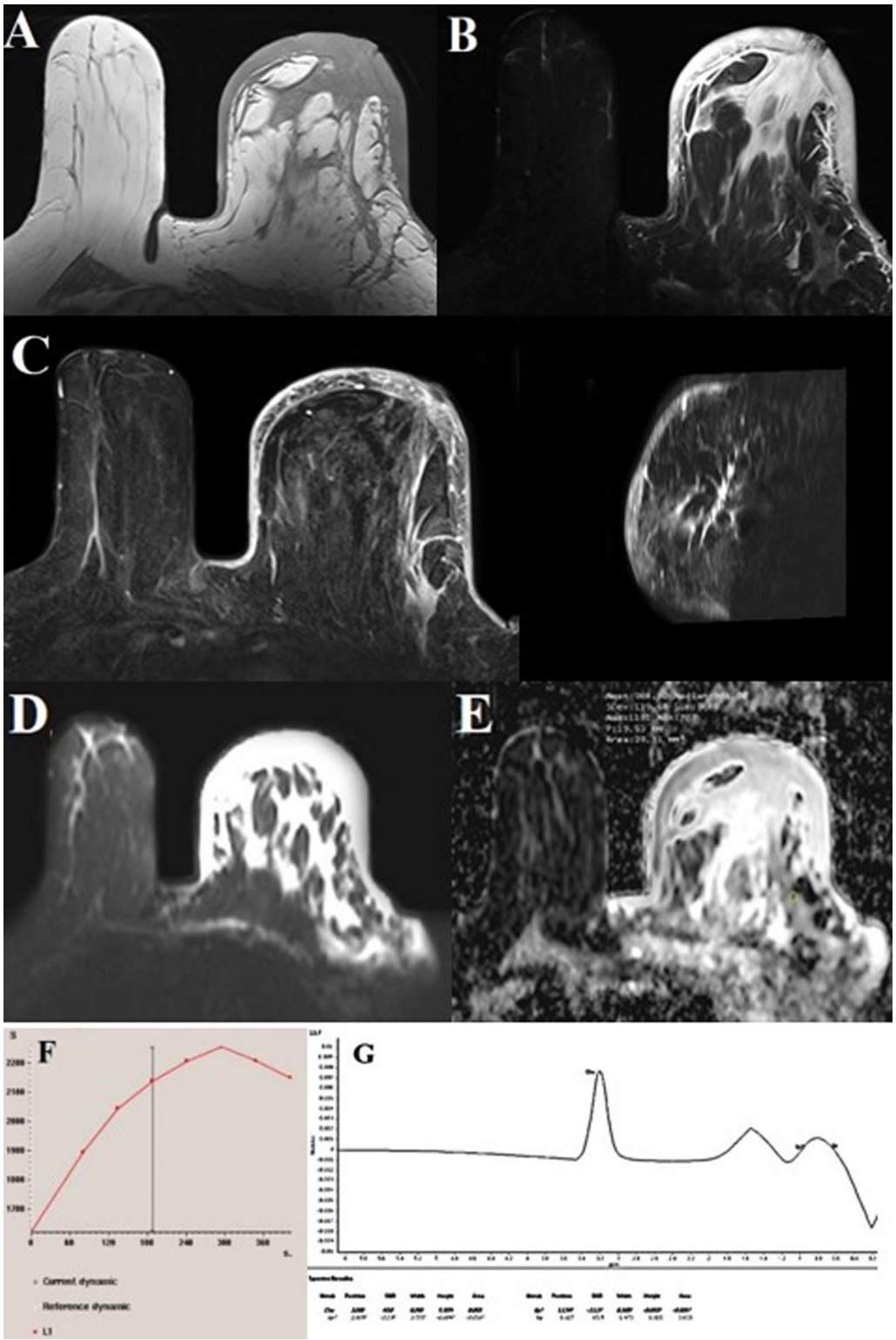

Fig. 4 (See legend on previous page.)

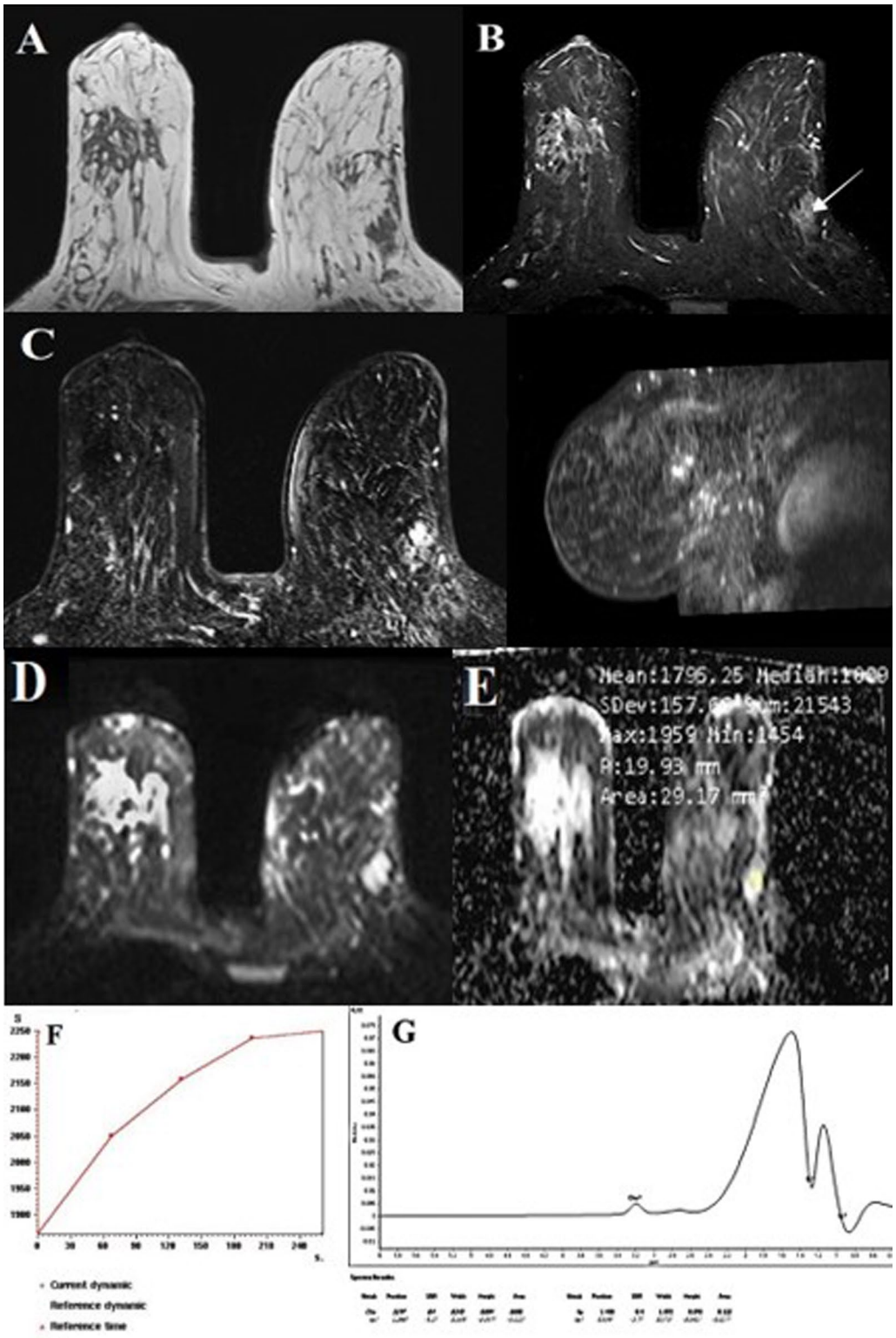

Fig. 5 Female patient aged 50 years old complaining from left mastalgia. MRI revealed: **A** Pre-contrast T1-weighted axial image showing: non-circumscribed area of low signal intensity seen at upper outer quadrant (UOQ) of left breast. **B** STIR axial image showing: an ill-defined area of high signal intensity is seen at UOQ of left breast. **C** Post-contrast subtraction axial and sagittal images showing segmental homogeneous non-mass enhancement with focal distribution is seen at UOQ of left breast. **D** and **E** DWI show high signal and high signal in ADC map with mean ADC value = 1.7×10^{-3} mm/s. **F** The enhancement kinetic curve of the lesion shows progressive enhancement type I curve.**G** MRS revealed negative choline peak. Pathology proved to be Localized fibrocystic changes with scattered foci of apocrine metaplasia

Table 2 Histopathologic categories of non-mass enhancement lesion

Parameter	Frequency (%)
Histopathological type of benign lesions	
Fibrocystic disease	10(4.5%)
Inflammatory process	44(20%)
Histopathological type of malignant lesions	
Lobular carcinoma in situ (LCIS)	14(6.4%)
Invasive lobular carcinoma (ILC)	20(9.1%)
Invasive ductal carcinoma (IDC) with ductal carcinoma in situ (DCIS)	93(42.3%)
Ductal carcinoma in situ (DCIS)	39(17.7%)

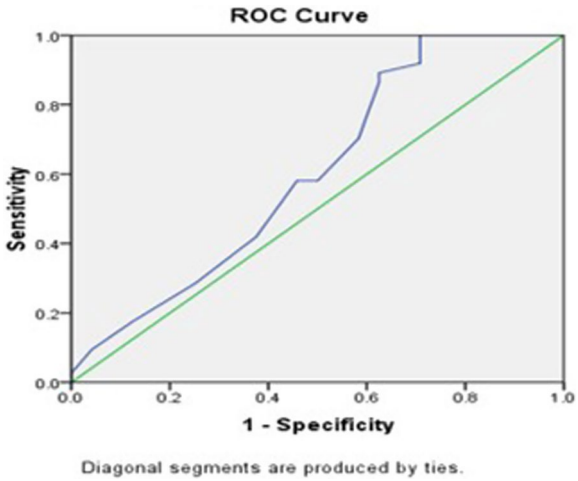

Fig. 6 Reciever Operating characteristics curve for ADC in differentiating between benign and malignant cases. It demonstrates that ADC cutoff value of $\leq 1.15 \times 10^{-3}$ has a good accuracy (AUC = 0.606, 70.3% sensitivity and 41.7% specificity) in discriminating malignant from benign lesions. ADC: Apparent diffusion coefficient, AUC: area under curve

agreed with Lunkiewicz and colleagues, who found that the pattern of segmental distribution is significantly more commonly detected in malignant lesions compared to other non-mass enhancement descriptors. [18, 21–23].

Our study investigated the enhancement patterns of non-mass enhancing lesions and found that heterogeneous enhancement was the most common enhancement

Table 3 MR characteristics of benign versus malignant non-mass enhancing lesions

Parameter	Benign (N = 54)	Malignant (N = 166)	Test of significance
Distribution			
Regional	7(13%)	52(31.3%)	$\chi^2 = 7.0$, $P = 0.008$*
Segmental	9(16.7%)	69(41.6%)	$\chi^2 = 10.57$, $P = 0.001$*
Multiple regions	11(20.4%)	0	$\chi^2 = 35.59$, $P = 0.001$*
Linear	13(24.1%)	9(5.4%)	$\chi^2 = 1.84$, $P = 0.17$
Focal	6(11%)	13(7.8%)	$\chi^2 = 0.81$, $P = 0.365$
Diffuse	8(14.8%)	23(13.9%)	$\chi^2 = 4.62$, $P = 0.03$
Enhancement patterns			
Homogenous	35(65.3%)	61(36.7%)	$\chi^2 = 3.87$, $P = 0.12$
Heterogeneous	16(28.8%)	75(45.2%)	$\chi^2 = 1.76$, $P = 0.185$
Clustered	0	11(6.6%)	$\chi^2 = 32.21$, $P = 0.001$*
Clumped	3(5.9%)	19(11.5%)	$\chi^2 = 2.51$, $P = 0.171$
Type of signal/intensity curve			
Type I	36(66.7%)	22(13.3%)	$\chi^2 = 2.19$, $P = 0.08$
Type II	14(25.9%)	47(28.3%)	$\chi^2 = 1.87$, $P = 0.06$
Type III	4(7.4%)	97(58.4%)	$\chi^2 = 1.12$, $P = 0.02$*
Diffusion			
Low signal	16(29.6%)	21(12.7%)	$\chi^2 = 8.39$, $P = 0.004$*
High signal	38(70.4%)	145(87.3%)	
ADC			
Value	1.26 ± 0.37	1.03 ± 0.278	t = 4.05, $P = 0.001$*
MRS			
Negative choline peak	39(72.2%)	24(14.5%)	$\chi^2 = 66.53$, $P < 0.001$*
Positive choline peak	15(27.8%)	142(85.5%)	

ADC Apparent diffusion coefficient, *MRS* Magnetic resonance spectroscopy, *t* Student's t test, χ^2 Chi-Square test, *P* Probability, *statistically significant

Table 4 Validity of various MR sequences in predicting malignant non-mass enhancement lesions

Parameter	Sensitivity%	Specificity%	PPV%	NPV%	Accuracy%
DCE-MRI	86.1	96.3	98.6	69.3	88.6
DWI	87.8	33.3	80.2	47.1	74.5
ADC	70.3	41.7	78.8	31.2	63.3
MRS	85.5	72.2	90.4	61.9	82.3
Combined (DWI, ADC, and MRS)	85.5	83.3	94.0	65.2	85
Mp-MRI (DCE-MRI, ADC, DWI and MRS)	89.9	87.8	89.2	82.2	91.2

DCE-MRI Dynamic contrast enhancement-magnetic resonance imaging, *DWI* Diffusion-weighted imaging, *ADC* Apparent diffusion coefficient, *MRS* Magnetic resonance spectroscopy, *Mp-MRI* Multiparametric-magnetic resonance imaging, *PPV* Positive predictive value, *NPV* Negative predictive value

seen in malignant lesions, with a prevalence of 45.2% (75/166) and a PPV of 65.4%. In addition, clustered ring enhancement was found exclusively in malignant lesions ($P=0.001$). These findings are consistent with the results reported by Cho and colleagues, who also found that heterogeneous enhancement was the prevalent feature in malignant non-mass enhancing lesions, with a prevalence of 45.2% and a PPV of 78.6%. Moreover, all non-mass enhancing lesions showing clustered ring enhancement were diagnosed as malignant. Our results are also in agreement with Tozaki and colleagues, who reported that the most common characteristic feature seen in malignant lesions was heterogeneous pattern of enhancement (69%) ($P=0.003$). Interestingly, the clustered ring pattern of enhancement was detected at 63% of malignant NME lesions and only 4% of benign NME lesions ($P<0.001$). We found that clustered ring enhancement was only in malignant lesions ($P=0.001$). Hande and colleagues reported that clustered ring enhancement can predict the probability of malignancy for non-mass enhancing lesions. Also, Kunimatsu and colleagues reported that pattern of clustered ring enhancement is widely detected morphologic feature of DCIS on DCE-MRI [24–27].

Regarding benign non-mass enhancing lesions, our study found that the most common enhancement pattern was homogenous enhancement, which was observed in 65.3% (35/54) of cases. This finding is consistent with the results reported by Tezcan and colleagues who revealed that homogeneous enhancement (22/37) was more likely in benign lesions our result also agreed with Hande and coworkers, who also found that a homogenous enhancement pattern was a significant predictor of benign non-mass enhancing lesions [26, 28].

On dynamic curves, the washout type curve (type III) showed statistical significance between benign and malignant non-mass enhancing lesions ($P=0.02$). The washout type curve (type III) was frequently more observed in malignant cases (97/166, 58.4%) compared to the benign group (4/54, 7.4%). Conversely, the occurrence of the type I curve was more prevalent in benign lesions (36/54, 66.7%) than in malignant lesions (22/166, 13.3%), although the statistical significance was weaker ($P=0.08$). The time intensity curve model demonstrated a sensitivity of 97.3% and specificity of 88.9% in predicting malignant non-mass enhancing lesions. These findings are consistent with a study done by Liu and colleagues who reported that washout curve (type III) was more associated with malignant lesions (28/56, 50%) in comparison with benign lesions (18/62, 29%) These differences in the occurrence of the washout type curve (type III) were statistically significant in both benign and malignant non-mass enhancing lesions, with a p value of less than 0.05. Similarly, the presence of type I curve was more detected at benign NME lesions (18/62, 29%) in comparison with malignant lesions (2/56, 3.6%) [$P=0.02$]. In that study as well, the sensitivity and specificity of the time intensity curve model for detecting the malignant nature of NME lesions were reported as 96.4% and 29.0%, respectively [18].

Regarding diffusion-weighted imaging (DWI), the random movement (Brownian motion) of water molecules throughout body tissue can be detected and calculated by measuring the apparent diffusion coefficient value (ADC). Malignant lesions will normally exhibit restriction in the diffusion ability of their water molecule and subsequently will display high signal intensity on diffusion weight images and low signal intensity on ADC maps as result of increase cellular density and this with result in extracellular space compression and changes of their microstructure [29].

In our research work, we detected that DWI and ADC value parameters were crucial in differentiating between malignant and benign non-mass enhancing lesions. The incidence of diffusion restriction in malignant non-mass enhancing lesions was significantly more than that detected at benign non-mass enhancing lesions with ($P=0.004$), and with sensitivity = 87.8%, specificity = 33.3%, PPV = 80.2%, accuracy = 74.5%, and this was in line with Marino and coworkers who reported that the sensitivity and specificity of the DWI in predicting malignant non-mass enhancing lesions were 74.36% and 66.66% and PPV = 76.34%, accuracy = 71.28% [10].

In the current study, the area under ROC curve of ADC in differentiating malignant from benign lesions = 0.606(0.462–0.750), P value = 0.121, cutoff point = 1.15, sensitivity = 70.3%, specificity = 41.7%, PPV = 78.8%, NPV = 31.2%,

accuracy=63.3%, in line with Marino and colleagues who reported that area under ROC curve=0.753(0.586–0.816), *P* value≤0.001, cutoff point=1.215, sensitivity=74.36%, specificity=66.66%, PPV=76.34%, NPV=64.24%, accuracy=71.28% [10].

Regarding ADC values, we found that malignant non-mass enhancing lesions more commonly showed lower ADC values ($\leq 1.03\times10^{-3}$ mm^2/s) compared with benign lesions. This difference is significant statistically ($P=0.002$) which is consistent with Avendano and colleagues who reported that benign non-mass lesions typically have a mean ADC value greater than $1.3\times10^{-3}\,mm^2/s$, while malignant non-mass lesions have a mean ADC value of $\leq 1.3\times10^{-3}mm^2/s$. [30].

Magnetic resonance spectroscopy (MRS) is incorporated in MRI techniques to evaluate the presence of an elevated choline (Cho) signal, that results from several Cho-containing compounds; such as free choline, phospho-choline, and glycerol-phospho-choline. This Cho peak is specified as total Cho and is believed to happen as result of increased levels of phospho-choline intracellularly as well as increased cell density that occurs in breast cancer [29]. In our evaluation of the clinical utility of MRS, the presence of composite Cho compounds was used as an indicator of malignancy, whereas their absence indicates a benign lesion.

The MRS findings in our study showed a statistically significant difference between the two groups, with a positive choline peak being more common among the malignant group. Out of 166 cases of malignant non-mass enhancing lesions, 142(85.5%) showed a positive choline peak, which was significantly higher compared to the benign group ($P<0.001$). The sensitivity of the positive choline peak for detecting malignancy was 85.5%, specificity was 72.2%, positive predictive value (PPV) was 90.4%, and overall accuracy was 82.3%. However, these results were not as high as those reported in a previous study by Bartella and coworkers, as his study included 32 cases non-mass enhancing lesions on MRI, of which 12 (37%) were malignant and 20 were benign. He found that a positive choline peak was detected in all cases of malignant non-mass enhancing lesions, with a sensitivity of 100% and a specificity of 85%. The difference in the results can be attributed to variations in breast cancer histology, and the sensitivity of breast MRS was also affected by false negative findings in different histological types. Additionally, the study by Bartella included fewer cases of ductal carcinoma in situ (DCIS) lesions (17%) as compared to the current study. In contrast, Tozaki and colleagues reported that MRS was not a powerful method for characterizing non-mass enhancing lesions [31, 32].

After analyzing 220 breast lesions, we confirmed that multiparametric-MRI (Mp-MRI) had superior diagnostic performance relative to DCE-MRI alone for discriminating benign and malignant non-mass enhancing lesions. The diagnostic accuracy of the DCE-MRI model was 88.6%. The sensitivity, specificity, PPV, and NPV were 86.1%, 96.3%, 98.6%, and 69.3%, respectively, this was based on the combination of enhancement pattern and kinetic criteria. And the diagnostic accuracy of combined functional MRI techniques (DWI, ADC, and MRS) without DCE-MRI was 85% with a sensitivity of 85.5%, specificity of 83.3%, PPV of 94%, and NPV of 65.2%. On the other hand, the Mp-MRI model demonstrated a remarkable improvement with an accuracy of 91.2%, along with a sensitivity of 89.9%, specificity of 87.8%, PPV of 89.2%, and NPV of 82.2%. These findings align with a study conducted by Zang and colleagues, which investigated the diagnostic ability of dynamic contrast-enhanced MRI and Mp-MRI for distinguishing non-mass enhancing lesions. Their analysis of 199 non-mass enhancing breast lesions also concluded that Mp-MRI surpassed DCE-MRI technique alone in terms of diagnostic accuracy [33].

Conclusions

Functional MRI techniques, such as diffusion-weighted imaging and magnetic resonance spectroscopy, can provide helpful information in the assessment of non-mass enhancing breast lesions. They have high diagnostic accuracy, sensitivity, and specificity in characterizing non-mass enhancement breast lesions as benign or malignant. However, DCE-MRI is mandatory for lesion characterization and delineation of its nature and cannot be replaced by them alone in cases of lesion visualization. So, multiparametric-MRI can improve the diagnostic accuracy of non-mass enhancement breast lesions when combined with dynamic contrast-enhanced MRI and can help in reducing negative biopsy rates.

Limitations

The overall malignant rate is high and with a low rate of benign lesions. This is because our study population included only cases that had a clinical indication for breast MRI. This study did not include a variety of benign pathological entities such as atypical ductal hyperplasia, duct papilloma, or radial scar. The reproducibility of ADC values between MR pulse sequences is still questionable. However, optimal sites selection for data sampling and localization of ROIs would affect the consistent/unchanging acquisition of reliable ADC values.

Abbreviations

MRI	Magnetic resonance imaging
DCE-MRI	Dynamic contrast-enhanced magnetic resonance imaging
US	Ultrasound
DWI	Diffusion-weighted imaging
MRS	Magnetic resonance spectroscopy
tCho	Total choline

Mp-MRI	Multiparametric-magnetic resonance imaging
NME	Non-mass enhancement
BI-RADS	Breast imaging reporting and data system
US-CNB	Ultrasound-guided core needle biopsy
STIR	Short tau spin echo
SE EPI	Spin echo planner imaging
ADC	Apparent diffusion coefficient
GRE	Gradient
FAT-SAT	Fat saturation
PRESS	Point Resolved Spectroscopy Sequence
TR	Repetition time
TE	Time to echo
MIP	Maximum intensity projection
Cho	Choline
ROI	Region of interest
SPSS	Statistical package for social science
SD	Standard deviation
ROC	Receiver operating characteristic curve
P	Probability
PPV	Positive predictive value.
NPV	Negative predictive value.
IDC	Invasive ductal carcinoma
DCIS	Ductal carcinoma in situ
ILC	Invasive lobular carcinoma
LCIS	Lobular carcinoma in situ

Supplementary Information

The online version contains supplementary material available at https://doi.org/10.1186/s43055-024-01267-2.

Supplementary material 1.

Acknowledgements
We are grateful to our patients who accepted to participate in our study.

Author contributions
All authors have read & approved the manuscript. The study concept and design were proposed by DB & AE. FS & RK were involved in statistical analysis of data. AE & FS helped in writing the original manuscript. AE, RK &DB were involved in preparing figures and tables. AE, FS & DB helped in revision of the manuscript for important intellectual content.

Funding
The authors state that this work has not received any funding.

Availability of data and materials
All the scientific data are available and presented in the manuscript. The source data are available from the corresponding author on reasonable request.

Declarations

Ethics approval and consent to participate
Written informed consent was waived by the Institutional Review Board (IRB), Institutional Review Board (IRB) was obtained, IRB approval: R.24.02.2523.

Consent for publication
All the patients were consented and informed of possible research publication. All authors hereby confirm that all the copyrights if such work will be accepted in the Egyptian Journal of Radiology and Nuclear Medicine (EJRNM).

Competing interests
The authors declare that they have no competing interests.

Author details
[1]Department of Radiology, Faculty of Medicine, Mansoura University, Mansoura, Egypt.

Received: 1 March 2024 Accepted: 3 May 2024
Published online: 13 May 2024

References

1. Ebrahim YG, Louis MR, Ali E (2018) Multi-parametric dynamic contrast enhanced MRI, diffusion-weighted MRI and proton-MRS in differentiation of benign and malignant breast lesions: Imaging interpretation and radiology-pathology correlation. Egypt J Radiol Nucl Med 49(4):1175–1181
2. Kim HR, Jung HK (2018) Histopathology findings of non-mass cancers on breast ultrasound. Acta Radiologica Open 7(6):2058460118774957
3. Lee J, Lee JH, Baik S, Cho E, Won-Kim D, Kwon HJ, Kim EK (2016) Non-mass lesions on screening breast ultrasound. Med Ultrason 18(4):446–451
4. Ayatollahi F, Shokouhi SB, Teuwen J (2020) Differentiating benign and malignant mass and non-mass lesions in breast DCE-MRI using normalized frequency-based features. Int J Comput Assist Radiol Surg 15(2):297–307
5. Lee JM, Arao RF, Sprague BL, Kerlikowske K, Lehman CD, Smith RA et al (2019) Performance of screening ultrasonography as an adjunct to screening mammography in women across the spectrum of breast cancer risk. JAMA Internal Medicine 179(5):658–667
6. Krammer J, Pinker-Domenig K, Robson ME et al (2017) Breast cancer detection and tumor characteristics in BRCA1 and BRCA2 mutation carriers. Breast Cancer Res Treat 163(3):565–571
7. Kuhl CK, Strobel K, Bieling H et al (2017) Supplemental breast MR imaging screening of women with average risk of breast cancer. Radiology 283(2):361–370
8. Yang Q-X, Ji X, Feng L-L, Zheng L, Zhou X-Q, Qian W, Chen X (2017) To explore and evaluate new malignant predictors of breast non-mass enhancement lesions using the new BI-RADS MRI lexicon. J Xray Sci Technol 25(6):1033–1044
9. Iima M, Le Bihan D (2016) Clinical intravoxel incoherent motion and diffusion MR imaging: past, present, and future. Radiology 278(1):13–32
10. Marino MA, Avendano D, Sevilimedu V, Thakur S, Martinez D, Gullo RL et al (2022) Limited value of multiparametric MRI with dynamic contrast-enhanced and diffusion-weighted imaging in non-mass enhancing breast tumors. Eur J Radiol 156:110523
11. Zaric O, Pinker K, Zbyn S, Strasser B, Robinson S, Minarikova L et al (2016) Quantitative sodium MR imaging at 7 T: initial results and comparison with diffusion-weighted imaging in patients with breast tumors. Radiology 280(1):39–48
12. Sharma U, Agarwal K, Hari S, Mathur SR, Seenu V, Parshad R, Jagannathan NR (2019) Role of diffusion weighted imaging and magnetic resonance spectroscopy in breast cancer patients with indeterminate dynamic contrast enhanced magnetic resonance imaging findings. Magn Reson Imag 61:66–72
13. Zaky M, Bayoumi D, Ibrahim DA, Abdallah A (2019) Role of magnetic resonance spectroscopic imaging in recategorization of BIRADS 4 Breast Lesions. Med J Cairo Univers 87(September):3353–3364
14. Bhushan A, Gonsalves A, Menon JU (2021) Current state of breast cancer diagnosis, treatment, and theranostics. Pharmaceutics 13(5):723
15. Gilbert FJ, Pinker-Domenig K (2019) Diagnosis and staging of breast cancer: when and how to use mammography, tomosynthesis, ultrasound, contrast-enhanced mammography, and magnetic resonance imaging. Diseases of the Chest, Breast, Heart and Vessels 2019-2022. Diagnostic and interventional imaging. Springer, Cham, pp 155–166
16. Fardanesh R, Marino MA, Avendano D, Leithner D, Pinker K, Thakur SB (2019) Proton MR spectroscopy in the breast: technical innovations and clinical applications. J Magn Reson Imaging 50(4):1033–1046
17. Park JW, Ko KH, Kim EK, Kuzmiak CM, Jung HK (2017) Non-mass breast lesions on ultrasound: final outcomes and predictors of malignancy. Acta Radiol 58(9):1054–1060
18. Liu G, Li Y, Chen SL, Chen Q (2022) Non-mass enhancement breast lesions: MRI findings and associations with malignancy. Annals Translat Med. https://doi.org/10.21037/atm-22-503
19. Huang K, Dufresne M, Baksh M, Nussbaum S, Abbaszadeh Kasbi A, Mohammed A et al (2023) How Well Does Non-mass enhancement correlate with DCIS/invasive cancer? American Surgeon. https://doi.org/10.1177/00031348231156776

20. Mori N, Sheth D, Abe H (2020) Nonmass enhancement breast lesions: diagnostic performance of kinetic assessment on ultrafast and standard dynamic contrast-enhanced MRI in comparison with morphologic evaluation. Am J Roentgenol 215(2):511–518
21. Asada T, Yamada T, Kanemaki Y, Fujiwara K, Okamoto S, Nakajima Y (2018) Grading system to categorize breast MRI using BI-RADS 5th edition: a statistical study of non-mass enhancement descriptors in terms of probability of malignancy. Jpn J Radiol 36:200–208
22. Aydin H (2019) The MRI characteristics of non-mass enhancement lesions of the breast: associations with malignancy. Br J Radiol 92(1096):20180464
23. Lunkiewicz M, Forte S, Freiwald B, Singer G, Leo C, Kubik-Huch RA (2020) Interobserver variability and likelihood of malignancy for fifth edition BI-RADS MRI descriptors in non-mass breast lesions. Eur Radiol 30:77–86
24. Cho YH, Cho KR, Park EK, Seo BK, Woo OH, Cho SB, Bae JW (2016) Significance of additional non-mass enhancement in patients with breast cancer on preoperative 3T dynamic contrast enhanced MRI of the breast. Iran J Radiol. https://doi.org/10.5812/iranjradiol.30909
25. Tozaki M, Igarashi T, Fukuda K (2006) Breast MRI using the VIBE sequence: clustered ring enhancement in the differential diagnosis of lesions showing non-masslike enhancement. Am J Roentgenol-New Series- 187(2):313
26. Hande UU, Tosun M, Arslan AS (2022) Non-mass enhancement of breast MRI: the comparison of benign and malignant pathological diagnosis and association of internal enhancement pattern and distribution with breast cancer molecular sub-types. Acta Medica Nicomedia 5(3):165–171
27. Kunimatsu N, Kunimatsu A, Uchida Y, Mori I, Kiryu S (2022) Whole-lesion histogram analysis of apparent diffusion coefficient for the assessment of non-mass enhancement lesions on breast MRI. J Clin Imag Sci. https://doi.org/10.25259/JCIS_201_2021
28. Tezcan S, Ozturk FU, Uslu N, Akcay EY (2021) The role of combined diffusion-weighted imaging and dynamic contrast-enhanced MRI for differentiating malignant from benign breast lesions presenting washout curve. Can Assoc Radiol J 72(3):460–469
29. Leithner D, Wengert GJ, Helbich TH, Thakur S, Ochoa-Albiztegui RE, Morris EA, Pinker K (2018) Clinical role of breast MRI now and going forward. Clin Radiol 73(8):700–714
30. Avendano D, Marino MA, Leithner D, Thakur S, Bernard-Davila B, Martinez DF et al (2019) Limited role of DWI with apparent diffusion coefficient mapping in breast lesions presenting as non-mass enhancement on dynamic contrast-enhanced MRI. Breast Cancer Res 21:1–10
31. Bartella L, Thakur SB, Morris EA, Dershaw DD, Huang W, Chough E et al (2007) Enhancing nonmass lesions in the breast: evaluation with proton (1 H) MR spectroscopy. Radiology 245(1):80–87
32. Tozaki M, Fukuma E (2009) 1H MR spectroscopy and diffusion-weighted imaging of the breast: are they useful tools for characterizing breast lesions before biopsy? Am J Roentgenol 193(3):840–849
33. Zang H, Liu HL, Zhu LY, Wang X, Wei LM, Lou JJ et al (2022) Diagnostic performance of DCE-MRI, multiparametric MRI and multimodality imaging for discrimination of breast non-mass-like enhancement lesions. Br J Radiol 95(1136):20220211

Publisher's Note